

# Sputtered Nb- and Ta-doped TiO<sub>2</sub> transparent conducting oxide films on glass

Meagen A. Gillispie

National Renewable Energy Laboratory, Golden, Colorado, 80401; and Iowa State University, Ames, Iowa, 50011

Maikel F.A.M. van Hest, Matthew S. Dabney, John D. Perkins,<sup>a)</sup> and David S. Ginley<sup>b)</sup>  
National Renewable Energy Laboratory, Golden, Colorado, 80401

(Received 30 May 2007; accepted 5 June 2007)

Radio frequency (rf) magnetron sputtering is used to deposit Ti<sub>0.85</sub>Nb<sub>0.15</sub>O<sub>2</sub> and Ti<sub>0.8</sub>Ta<sub>0.2</sub>O<sub>2</sub> films on glass substrates at substrate temperatures ( $T_s$ ) ranging from ~250 to 400 °C. The most conducting Nb-doped TiO<sub>2</sub> films were deposited at  $T_s = 370$  °C, with conductivities of ~60 S/cm, carrier concentrations of  $1.5 \times 10^{21}$  cm<sup>-3</sup> and mobilities <1 cm<sup>2</sup>/V·s. The conductivity of the films was limited by the mobility, which was more than 10 times lower than the mobility for films deposited epitaxially on SrTiO<sub>3</sub>. The difference in properties is likely caused by the randomly oriented crystal structure of the films deposited on glass compared with biaxially textured films deposited on SrTiO<sub>3</sub>. The anatase phase could not be stabilized in the Ta-doped TiO<sub>2</sub> films, likely because of the high dopant concentration.

## I. INTRODUCTION

Transparent conducting oxides (TCOs) can conduct electricity while maintaining transparency in the visible region of the electromagnetic spectrum. Because of this, TCOs find application in a wide variety of devices including electrochromic windows, solar cells, light-emitting diodes, window deicers, and flat panel displays.<sup>1–5</sup> One of the key driving forces for developing new TCO materials is the ever-increasing cost of indium, a major component of the most widely used TCO, Sn-doped In<sub>2</sub>O<sub>3</sub>, commonly referred to as indium–tin–oxide (ITO). Hence, there is an increasing amount of attention on developing new reduced-In or In-free TCO materials that can perform as well as—if not better than—ITO, which typically possesses conductivity,  $\sigma$ , on the order of  $10^3$  to  $10^4$  S/cm and mobility,  $\mu$ , on the order of 25 to 35 cm<sup>2</sup>/V·s.<sup>6–8</sup> Doped SnO<sub>2</sub> and ZnO are two widely used In-free TCOs for low-emittance (low-e) windows and are being looked at for other applications.<sup>2,9,10</sup> While they do possess optoelectronic performance characteristics close to ITO, they also have significant drawbacks in their non-TCO properties such as deposition parameters

and chemical stability. As a result, there is a growing research thrust on further expanding the TCO landscape to look for new In-free materials outside the constellation of typical TCOs.

Recently Nb- or Ta-doped anatase TiO<sub>2</sub> has been identified as a viable TCO material.<sup>11–13</sup> Nb-doped TiO<sub>2</sub> films grown on strontium titanate single crystals SrTiO<sub>3</sub> (STO) by pulsed laser deposition (PLD) were shown to have conductivities on the order of 2 to  $4 \times 10^3$  S/cm and Hall mobilities,  $\mu_H$ , of 15 to 22 cm<sup>2</sup>/V·s at dopant concentrations of 3 to 6 mol% Nb.<sup>11,12</sup> Surprisingly, conductivity remained on the order of  $10^3$  S/cm for dopant concentrations as high as 20 mol%, although transparency decreased significantly. Ta-doped TiO<sub>2</sub> PLD films on STO were found to have similar electrical and optical properties for Ta dopant concentrations up to 15 mol%.<sup>13</sup> While possible substitutional donor dopants for Ti in anatase could include nearly all 5+ transition metals (particularly V, Nb, and Ta), the incorporation of V into TiO<sub>2</sub> has proven to be more difficult than Nb and Ta because of problems controlling stoichiometry in deposited films, most likely the result of metal oxide instability.<sup>14</sup>

To date, the best-performing TiO<sub>2</sub>-based TCOs were fabricated using epitaxial deposition by pulsed laser deposition on single-crystal substrates such as STO. In this paper, the structural, electrical, and optical properties of radio frequency (rf) magnetron sputtered Nb- and Ta-doped TiO<sub>2</sub> films on glass substrates are reported in exploration of the viability of doped TiO<sub>2</sub> as a practical TCO. The use of low-cost sputtering techniques to

<sup>a)</sup>Address all correspondence to this author.

e-mail: john\_perkins@nrel.gov

<sup>b)</sup>This author was an editor of this journal during the review and decision stage. For the JMR policy on review and publication of manuscripts authored by editors, please refer to [http://www.mrs.org/jmr\\_policy](http://www.mrs.org/jmr_policy)

DOI: 10.1557/JMR.2007.0353

fabricate TCO films is preferable to more expensive small-area PLD, as is deposition on glass substrates such as for use in flat-panel displays. It was recently demonstrated that the original PLD results can be matched (maximum conductivity of 3000 S/cm) by rf magnetron sputtering on single-crystal SrTiO<sub>3</sub> substrates.<sup>15</sup> To evaluate the viability of anatase TiO<sub>2</sub> as a TCO, it is key to determine whether or not epitaxial single-crystal films are required to achieve reasonable performance.

For the Nb-doped TiO<sub>2</sub> films on various substrates, the highest conductivity results were attained for films composed of anatase TiO<sub>2</sub>. Anatase TiO<sub>2</sub> (*I*<sub>4</sub>/amd) is one of three natural polymorphs of TiO<sub>2</sub>. It is typically a low-temperature metastable phase that exists in a tetragonal structure like the more stable polymorph rutile (*P*<sub>4</sub><sub>2</sub>/mmn), yet structural differences between the two give them each different electrical and optical properties. In anatase, TiO<sub>6</sub> octahedra are edge-sharing and form a spiral chain through the structure, whereas in rutile, the TiO<sub>6</sub> octahedra share corners. Of the two, anatase possesses a larger band gap ( $E_g = 3.2$  versus 3.0 eV for rutile) and smaller conduction band effective mass ( $m^* \sim 1 m_e$  versus  $m^* \sim 20 m_e$  for rutile), making anatase TiO<sub>2</sub> a better candidate for possible use as a TCO with high conductivity and transparency.<sup>16</sup>

In this work, rf magnetron sputtering is used to deposit Ti<sub>0.85</sub>Nb<sub>0.15</sub>O<sub>2</sub> and Ti<sub>0.8</sub>Ta<sub>0.2</sub>O<sub>2</sub> films on glass substrates at substrate temperatures ( $T_s$ ) ranging from ~250 to 400 °C. The most conducting Nb-doped TiO<sub>2</sub> films were deposited at  $T_s = 370$  °C, with conductivities of ~60 S/cm, carrier concentrations of  $1.5 \times 10^{21} \text{ cm}^{-3}$  and mobilities  $< 1 \text{ cm}^2/\text{V}\cdot\text{s}$ . The conductivity of the films on glass was more than 10 times lower than that for films deposited epitaxially on STO.<sup>15</sup> At present, this difference is attributed to the randomly oriented crystal structure of the films deposited on glass compared with biaxially textured films deposited on STO.

## II. EXPERIMENTAL

Nb-doped, Ta-doped, and undoped TiO<sub>2</sub> films were deposited onto 2 in.  $\times$  2 in. Corning 1737 glass substrates using 2 in. oxide targets consisting of pure TiO<sub>2</sub> (99.995%, Plasmaterials, Livermore, CA), 7.5 mol% Nb<sub>2</sub>O<sub>3</sub> in TiO<sub>2</sub> (Ti<sub>0.85</sub>Nb<sub>0.15</sub>O<sub>2+δ</sub>, 99.9%, Plasmaterials), and 10 mol% Ta<sub>2</sub>O<sub>5</sub> in TiO<sub>2</sub> (Ti<sub>0.8</sub>Ta<sub>0.2</sub>O<sub>2+δ</sub>, 99.95%, Plasmaterials). The sputtering system used for this investigation was arranged with a 2 in. sputtering gun (Angstrom Sciences Onyx 2 Magnetron Sputter Source, Duquesne, PA) positioned at a 45° angle to a stationary substrate holder with a resistive substrate heater capable of temperatures up to 900 °C. The target-to-substrate distance is 8 cm at the center of the target and substrate. This configuration results in a thickness gradient in a film deposited from a single target.

Films were deposited in pure argon (grade 5.0) at a flow rate of 20 sccm, at a system pressure of 4.5 mTorr, and with substrate temperatures ranging from about 250 to 400 °C to observe the phase evolution and stability. The RF-sputtering powers (Manitou Series PB-3 RF Power System) required to attain films with a thickness gradient of approximately 90 to 250 nm across the substrate surface after 1 h of deposition were 50, 30, and 25 W for the pure TiO<sub>2</sub>, Nb-doped TiO<sub>2</sub>, and Ta-doped TiO<sub>2</sub> targets, respectively.

Phase evolution and stability was examined using x-ray diffraction (XRD) with a two-dimensional detector (Bruker D8 Discover,). Conductivity, mobility, and carrier concentration were measured using a BioRad Hall measurement system. Optical transmission and reflection was analyzed over the wavelength range of 250 nm to 25 μm using a combination of Ocean Optics CCD and diode-array-based spectrometer in the ultraviolet (UV), visible (VIS), and near-infrared (NIR) and Fourier transform infrared (FTIR) spectroscopy beyond 1.5 μm.<sup>17</sup>

On each 2 in.  $\times$  2 in. film, XRD and four-point probe measurements were made over the entire surface in a 4-row by 11-column pattern, with the thickness gradient oriented along each row. In all cases, the side of the film that was closest to the sputter target during deposition possessed the lowest sheet resistance, with values increasing by orders of magnitude across the film surface from thick side to thin side. Variation in crystallinity was also observed across the thickness profile. In addition to solely thickness effects, the range of properties observed across the film surface could be due to variations in ion energy resulting from the sputtering geometry. All results presented in this paper are for a section approximately 9 mm  $\times$  9 mm cut from the thick side of each substrate. Approximate film thickness of each 9 mm  $\times$  9 mm piece was 200 nm, with a variation of ~15 nm across the surface due to the angled deposition.

## III. RESULTS AND DISCUSSION

Electrical properties of Nb-doped TiO<sub>2</sub> (15 mol%) films on glass are shown for all deposition temperatures in Fig. 1. The film deposited at 260 °C was not conductive enough for Hall measurements, so only the four-point probe conductivity [Fig. 1(a)] data is presented. For deposition temperatures below 350 °C, conductivity is fairly constant, at values less than 8 S/cm. At a deposition temperature of 370 °C, conductivity is significantly higher at 56 S/cm and begins to drop off again when substrate temperature is raised just 20 °C. The measurement error is about 30% for both mobility and carrier concentration, a result of the low mobility ( $< 1 \text{ cm}^2/\text{V}\cdot\text{s}$ ) observed in the films. A definite maximum in carrier concentration is observed over the range of deposition temperatures with the films deposited at 370

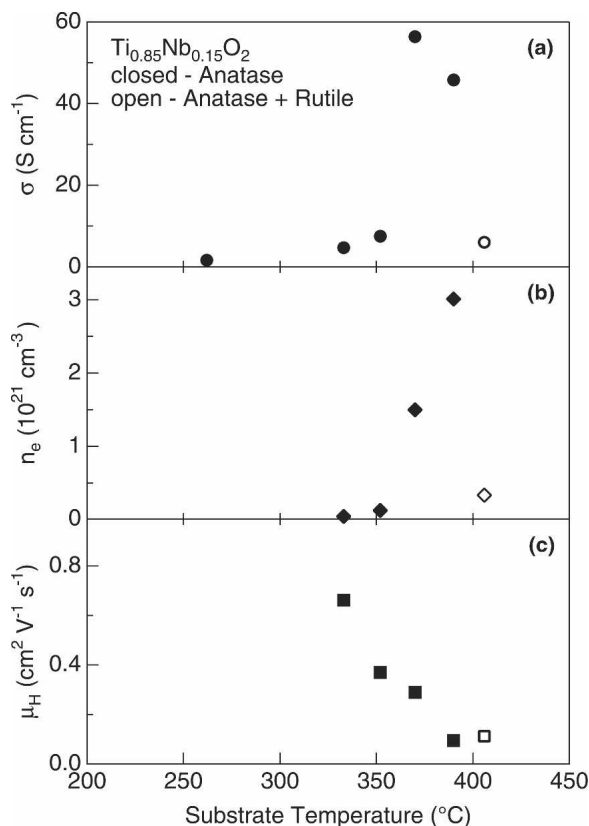


FIG. 1. Electrical properties of Ti<sub>0.85</sub>Nb<sub>0.15</sub>O<sub>2</sub> films deposited on glass at varying deposition temperatures. (a) Conductivity. (b) Carrier concentration. (c) Hall mobility. Closed symbols: anatase phase only. Open symbols: mixed anatase and rutile phases.

and 390 °C having carrier concentrations greater than 10<sup>21</sup> cm<sup>-3</sup>.

The highest observed conductivity for films on glass ( $\sigma = 56$  S/cm) was much lower than the conductivity observed for Nb-doped TiO<sub>2</sub> films deposited on STO using PLD ( $\sigma \approx 2$  to  $4 \times 10^3$  S/cm).<sup>11,12,15</sup> Values were also much lower than sputter-deposited films on single-crystal lattice matched substrates, which also showed  $\sigma \approx 2$  to  $4 \times 10^3$  S/cm.<sup>15</sup> This conductivity is an improvement over undoped TiO<sub>2</sub> sputtered on glass, which had a conductivity on the order of 10<sup>-2</sup> S/cm. Carrier concentration in the films is very high ( $\sim 10^{21}$  cm<sup>-3</sup>) and consistent with values for PLD and sputtered films on STO, yet the mobility is drastically different, about 10 times lower.

Figure 2 shows the XRD spectra for the temperature series of depositions. All peaks present could be attributed to either the anatase or rutile phase of TiO<sub>2</sub> except for one weak unidentified peak at  $2\theta = 30.8^\circ$  for the film grown at  $T_s = 352$  °C. The respective expected powder diffraction patterns and their  $hkl$  indices are shown in Figs. 2(b) and 2(c). The spectra in Fig. 2 show that for all deposition temperatures below 400 °C, anatase was the dominant phase present in the films. In these films, anatase is randomly oriented, as evidenced by the presence

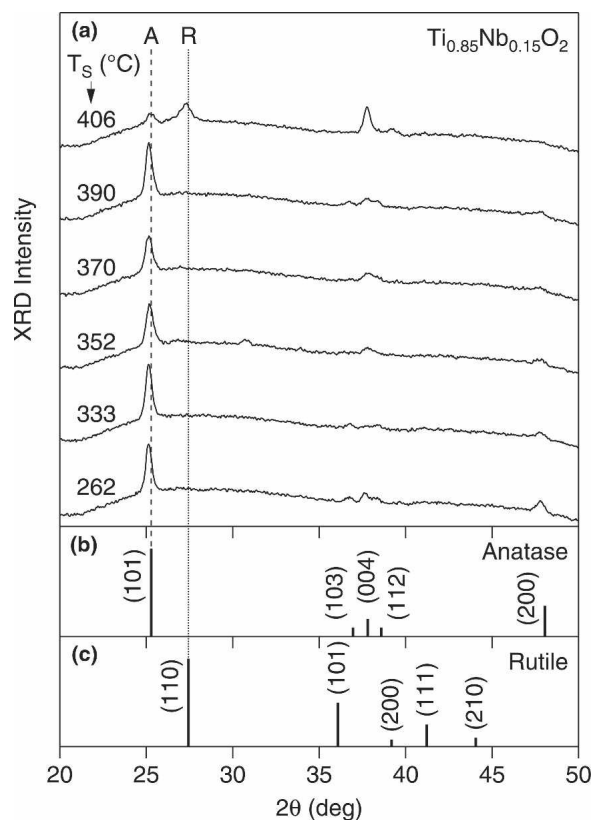


FIG. 2. (a) XRD spectra for Ti<sub>0.85</sub>Nb<sub>0.15</sub>O<sub>2</sub> films deposited on glass at various substrate temperatures ( $T_s$ ). (b) Expected powder diffraction pattern for anatase TiO<sub>2</sub> (JCPDS 21-1272). (c) Expected powder diffraction pattern for rutile TiO<sub>2</sub> (JCPDS 21-1276).

of multiple anatase peaks in many of the patterns. This result is in contrast with the epitaxial (004) anatase films deposited on (100) STO.<sup>11,12,15</sup>

The anatase-to-rutile transition is expected to occur anywhere between 400 and 1000 °C for undoped bulk TiO<sub>2</sub>. Doping in bulk TiO<sub>2</sub> with higher oxidation state cations, such as Nb<sup>5+</sup> for Ti<sup>4+</sup>, will shift the transition temperature lower.<sup>18,19</sup> For this reason, it is possible to observe the formation of rutile in films deposited at temperatures lower than 400 °C. Multiple films deposited at 390 °C contained varying amounts of anatase, as seen in Fig. 3, indicating that the conditions are favorable for the formation of rutile. This is further supported by the results for the film deposited at 406 °C, which shows rutile as the dominant phase present as can be seen in Fig. 2. Undoped films sputtered on glass at temperatures as high as 406 °C are composed of anatase only, as seen in Fig. 4. It should be noted that the anatase XRD pattern for this film is fairly weak compared with the Nb-doped TiO<sub>2</sub> films, indicating that the film is not very crystalline. The observations made here are in agreement with other reports of sputtered TiO<sub>2</sub> films, which showed the formation of anatase films at temperatures as high as 400 °C.<sup>16,20,21</sup> These results, along with the XRD spectra

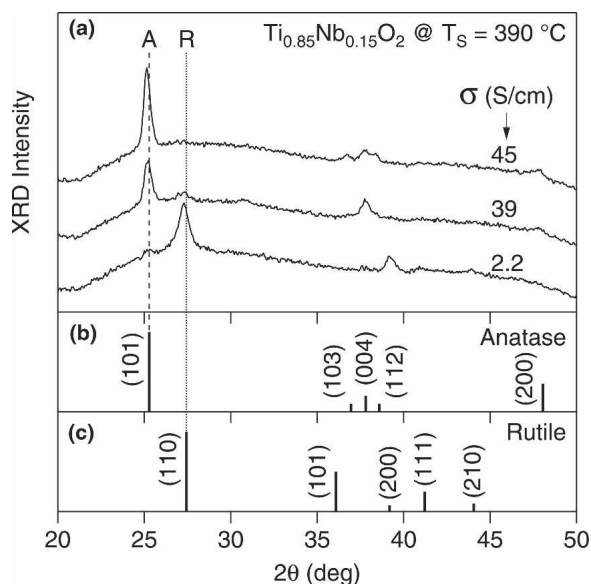


FIG. 3. (a) XRD spectra for  $\text{Ti}_{0.85}\text{Nb}_{0.15}\text{O}_2$  films deposited on glass at 390 °C. (b) Expected powder diffraction pattern for anatase  $\text{TiO}_2$  (JCPDS 21-1272). (c) Expected powder diffraction pattern for rutile  $\text{TiO}_2$  (JCPDS 21-1276).

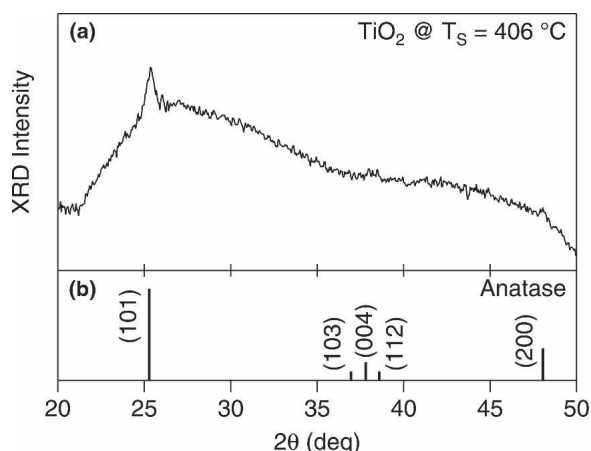


FIG. 4. (a) XRD spectrum for undoped  $\text{TiO}_2$  deposited on glass at a substrate temperature of 406 °C. (b) Expected powder diffraction pattern for anatase  $\text{TiO}_2$  (JCPDS 21-1272).

shown in Fig. 4, suggest that the anatase-to-rutile transition temperature for the deposition conditions used in this study is likely higher than 400 °C for pure  $\text{TiO}_2$ .

Ta-doped  $\text{TiO}_2$  (20 mol%) films deposited on glass were amorphous for substrate temperatures as high as 390 °C. When the substrate temperature was increased to 406 °C, the film crystallized directly to rutile  $\text{TiO}_2$ . XRD patterns for both deposition temperatures are given in Fig. 5. The XRD pattern for the film deposited at 390 °C is identical to the pattern for a bare glass substrate. It is likely that such a high Ta doping level (20 mol%) has the effect of both inhibiting crystallization and stabilizing rutile at lower temperatures, an effect that can be over-

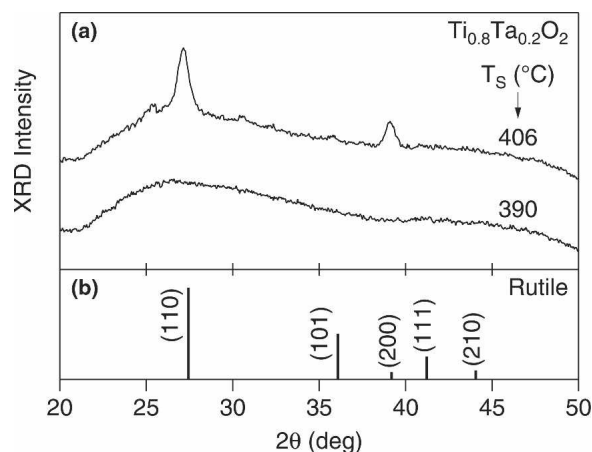


FIG. 5. (a) XRD spectra for  $\text{Ti}_{0.8}\text{Ta}_{0.2}\text{O}_2$  films deposited on glass at different substrate temperatures. (b) Expected powder diffraction pattern for rutile  $\text{TiO}_2$  (JCPDS 21-1276).

come by using an (100) STO substrate.<sup>15</sup> A similar crystallization phenomenon is observed in Zr-doped  $\text{Ta}_2\text{O}_5$  films, in which Zr additions of ~20 at.% increased the crystallization temperature by 100 °C.<sup>22</sup> There is some texturing in the rutile film deposited at 406 °C since the (101), (111), and (210) peaks are not present in the pattern and for a randomly oriented rutile film. All these peaks should be more intense than the (200) peak, but they are not, indicating some preferential (200) orientation.

Optical transmission and reflection spectra for the most-conductive Nb-doped  $\text{TiO}_2$  film,  $\sigma = 56$  S/cm deposited at 370 °C, are shown in Fig. 6. The reflection spectrum is measured relative to either an Al or Au mirror and corrected for the known reflectance of the reference mirror. The transmission spectrum as shown is normalized to the transmission of a bare glass substrate. There is a discontinuity in the measured transmission spectrum at ~0.78 eV, the crossover point to the FTIR

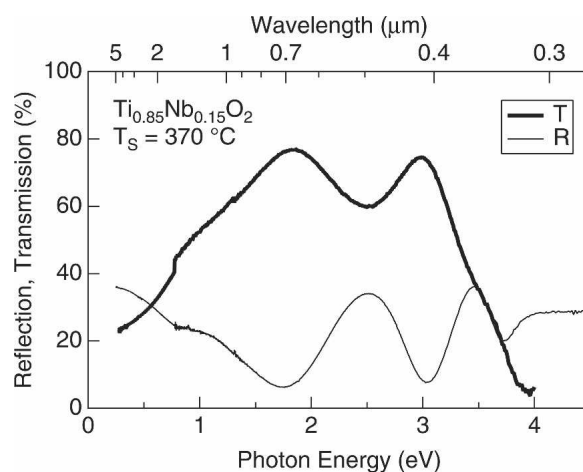


FIG. 6. Optical transmission and reflection spectra for a  $\text{Ti}_{0.85}\text{Nb}_{0.15}\text{O}_2$  film deposited on glass at 370 °C.



measured spectra. At photon energies ( $\hbar\omega$ ) higher than  $\sim 4$  eV and lower than  $\sim 0.3$  eV, the glass substrate is too opaque for transmission measurements.

The films are only 65% to 70% transparent with a visible bluish tint. For ( $\hbar\omega$ )  $< 1.5$  eV, the concurrent gradual decrease in transmission and increase in reflection with decreasing photon energy is indicative of optically excited plasma oscillations (Drude model) for a sample with high carrier concentrations and low mobility. In the Drude model, the crossover from transparent to reflecting with decreasing photon energy occurs at the plasma frequency which, expressed as a photon energy, is given by

$$\hbar\omega_p = h \sqrt{\frac{4\pi N e^2}{\epsilon_\infty m^*}}, \quad (1)$$

where  $c$  is the speed of light,  $\epsilon_\infty$  is the dielectric function in the visible,  $m^*$  is the electron,  $N$  is the free electron density, and  $e$  is the electron charge.<sup>17</sup> Taking  $\epsilon_\infty = 6.25$  and  $m^* = 1 m_e$  as appropriate for anatase TiO<sub>2</sub>,<sup>16</sup>  $N = 1.5 \times 10^{21} \text{ cm}^{-3}$  as measured here for the film deposited at 370 °C, gives  $\hbar\omega_p \approx 0.6$  eV, qualitatively consistent with the spectra shown in Fig. 6. In addition, the crossover from transparent to reflecting is very broad, occurring over about 1 eV in energy. This indicates a low mobility, consistent with the Hall effect data shown in Fig. 1 where  $\mu_H = 0.3 \text{ cm}^2/\text{V}\cdot\text{s}$  for this sample.

High doping levels and carrier concentrations are known to reduce the transparency of TiO<sub>2</sub> films in the visible portion of the electromagnetic spectrum, as is the case with these films.<sup>11,12</sup> This is likely due to the high carrier concentration ( $>10^{21} \text{ cm}^{-3}$ ) and the low mobility ( $\mu_H < 1 \text{ cm}^2/\text{V}\cdot\text{s}$ ) pushing the high-energy tail of the plasma oscillation effects into the visible spectrum. This same effect was observed by Furubayashi et al. in PLD Nb-doped TiO<sub>2</sub> films.<sup>11,12</sup> They found that lower dopant concentration and resulting lower carrier concentration gave more transparent films since the plasma edge red shifts with decreasing carrier concentration as  $\hbar\omega_p \propto \sqrt{n_e}$ . For this reason, it is likely that sputtered films on glass doped with much smaller amounts of Nb would have higher transparency in the visible part of the spectrum.

In Fig. 3, the measured conductivity of each 9 mm  $\times$  9 mm section of the film is also given along with the XRD patterns. In short, for these 200-nm-thick films, the stronger the rutile phase XRD scattering, the lower the conductivity. In particular, for the films of Fig. 3, the conductivity decreases from 45 S/cm for a film that is mostly anatase (top spectrum) to 2.2 S/cm for a mostly rutile film (bottom spectrum). These three films were all deposited at a nominal front surface substrate temperature of 390 °C. However, this reported temperature is determined from the substrate heater block temperature

and a one-time calibration of the corresponding substrate surface temperature using a thermocouple. Hence, it is likely that deposition-to-deposition variations in the true substrate surface temperature account for the observed variation in the crystalline phases and, in turn, the corresponding difference in electrical conductivity.

A similar reduced conductivity is also observed in the film deposited at 406 °C from Fig. 2, which contained both rutile and anatase phases and is plotted in Fig. 2 using an open symbol to emphasize this difference. By comparing relative peak intensity of the 100% anatase and rutile peaks (assuming 100% crystallinity for the maximum peak intensity of a phase-pure film), the film deposited at 406 °C was  $\sim 31\%$  anatase. For this film,  $\sigma = 6 \text{ S/cm}$ , almost 10 times lower than that for the anatase only film grown at 370 °C. Collectively, these results indicate that anatase is the dominant crystalline phase responsible for the high conductivity observed in all of the films.

The low measured conductivities of the films showing mixed rutile and anatase phases may be caused by percolative conduction predominately through the anatase grains. Thus, as the rutile volume fraction grows, the percolative pathways are increasingly disrupted. While this effect may exist in all films, it may also be that the high-angle grain boundaries in randomly oriented anatase films are far more resistive than the predominately low-angle boundaries in the biaxially textured films on single-crystal substrates such as STO. Note that for Ti<sub>0.85</sub>Nb<sub>0.15</sub>O<sub>2</sub> films grown in the same deposition system and under nearly identical conditions but on STO instead of on glass, the measured conductivity is  $\sim 3000 \text{ S/cm}$ , roughly 50 times higher than for the films grown on glass substrates.<sup>15</sup> Furthermore, for Ti<sub>0.85</sub>Nb<sub>0.15</sub>O<sub>2</sub> films grown on STO at  $T_s = 375$  °C, the Hall mobility  $\mu_H = 7.6 \text{ cm}^2/\text{V}\cdot\text{s}$ , whereas for the films grown on glass at  $T_s = 370$  °C,  $\mu_H = 0.3 \text{ cm}^2/\text{V}\cdot\text{s}$ , 25 times lower.

Hence, almost all of the decrease in conductivity for Ti<sub>0.85</sub>Nb<sub>0.15</sub>O<sub>2</sub> films grown on glass compared with those grown (100) STO substrates is due to a large increase in the scattering, not a decrease in the carrier concentration that could arise from a change in the effectiveness of the Nb as a dopant. Considering this along with the randomly oriented structure of the Ti<sub>0.85</sub>Nb<sub>0.15</sub>O<sub>2</sub> films on glass as opposed to the biaxially textured Ti<sub>0.85</sub>Nb<sub>0.15</sub>O<sub>2</sub> films on STO, suggests that grain-boundary scattering from high-angle grain boundaries is a likely cause for the low carrier mobility for Ti<sub>0.85</sub>Nb<sub>0.15</sub>O<sub>2</sub> films on glass. Such strong carrier scattering at randomly aligned grain boundaries could arise from poor electronic overlap across the grain boundary of the directional Ti 3d states that make up the conduction band in anatase TiO<sub>2</sub> compared with the isotropic s states that form the conduction band in conventional TCOs such as ITO.<sup>23</sup>

It should be noted that the doping level used here

(15 mol%) was much higher than the optimal Nb doping level for PLD films on STO (3 mol%). While higher Nb doping levels for films on STO deposited by PLD still possessed conductivity on the order of 1000 S/cm, it is possible that the doping level is too high for films deposited on glass. However, if the low mobility for the films on glass is caused by high-angle grain-boundary scattering, it seems unlikely that reducing the Nb dopant level will significantly reduce the grain-boundary scattering. To achieve  $r$  conductivity it may be that more oriented films will need to be grown on glass. For example, the use of a textured template layer could be an alternate way to stabilize a biaxially textured structure for sputtered thin films on glass and hence to obtain better electrical and optical properties. Alternatively, the use of ion-beam-assisted deposition (IBAD) could also help stabilize a biaxially textured structure on glass.

#### IV. CONCLUSIONS

Transparent conductive Ti<sub>0.85</sub>Nb<sub>0.15</sub>O<sub>2+δ</sub> anatase films were sputter-deposited on glass substrates. Optimal conductivity of ~60 S/cm can be achieved using a substrate temperature of 370 °C. XRD results suggest that the presence of fully crystalline anatase TiO<sub>2</sub> is essential for achieving this conductivity. The introduction of the rutile phase in the films caused conductivity to decrease significantly, likely due to disruption of percolative pathways through the anatase grains. Mobility in the randomly oriented crystalline films is low,  $\mu_H < 1$  cm<sup>2</sup>/V·s. In contrast, biaxially textured Nb-doped TiO<sub>2</sub> films on STO have approximately the same carrier concentration but mobility is much higher  $\mu_H \approx 8$  cm<sup>2</sup>/V·s, resulting in better conductivity. Taken together, this suggests that for randomly oriented anatase Nb-doped TiO<sub>2</sub> films on glass that grain boundaries may well be the dominant scattering source. The anatase phase of TiO<sub>2</sub> could not be obtained for Ti<sub>0.8</sub>Ta<sub>0.2</sub>O<sub>2+δ</sub> films sputter-deposited on glass. Further investigations on both doping optimization and grain orientation control are needed to determine if the TCO properties of doped TiO<sub>2</sub> on glass can be improved enough to make it a technologically practical TCO.

#### ACKNOWLEDGMENT

This work was supported by the Laboratory Directed Research and Development program at the National Renewable Energy Laboratory.

#### REFERENCES

1. D.S. Ginley and C. Bright: Transparent conducting oxides. *MRS Bull.* **25**, 15 (2000).
2. R.G. Gordon: Criteria for choosing transparent conductors. *MRS Bull.* **25**, 52 (2000).
3. G. Haacke: Transparent conducting coatings. *Ann. Rev. Mater. Sci.* **7**, 73 (1977).
4. H. Hosono, H. Ohta, M. Orita, K. Ueda, and M. Hirano: Frontier of transparent conductive oxide thin films. *Vacuum* **66**, 419 (2002).
5. H. Kawazoe, H. Yanagi, K. Ueda, and H. Hosono: Transparent  $p$ -type conducting oxides: design and fabrication of  $p$ - $n$  heterojunctions. *MRS Bull.* **25**, 28 (2000).
6. B.G. Lewis and D.C. Paine: Applications and processing of transparent conducting oxides. *MRS Bull.* **25**, 22 (2000).
7. O.N. Mryasov and A.J. Freeman: Electronic band structure of indium tin oxide and criteria for transparent conducting behavior. *Phys. Rev. B* **64**, 233111 (2001).
8. R.B.H. Tahar, T. Ban, Y. Ohya, and Y. Takahashi: Tin doped indium oxide thin films: Electrical properties. *J. Appl. Phys.* **83**, 2631 (1998).
9. C.M. Dai, C.S. Su, and D.S. Chuu: Growth of highly oriented tin oxide thin films by laser evaporation deposition. *Appl. Phys. Lett.* **57**, 1879 (1990).
10. T. Minami: New  $n$ -type transparent conducting oxides. *MRS Bull.* **25**, 38 (2000).
11. Y. Furubayashi, T. Hitosugi, Y. Yamamoto, Y. Hirose, G. Kinoda, K. Inaba, T. Shimada, and T. Hasegawa: Novel transparent conducting oxide: Anatase Ti<sub>1-x</sub>Nb<sub>x</sub>O<sub>2</sub>. *Thin Solid Films* **496**, 157 (2006).
12. Y. Furubayashi, T. Hitosugi, Y. Yamamoto, K. Inaba, G. Kinoda, Y. Hirose, T. Shimada, and T. Hasegawa: A transparent metal: Nb-doped anatase TiO<sub>2</sub>. *Appl. Phys. Lett.* **86**, 252101 (2005).
13. T. Hitosugi, Y. Furubayashi, A. Ueda, K. Itabashi, K. Inaba, Y. Hirose, G. Kinoda, Y. Yamamoto, T. Shimada, and T. Hasegawa: Ta-doped anatase TiO<sub>2</sub> epitaxial film as transparent conducting oxide. *Jpn. J. Appl. Phys.* **44**, L1063 (2005).
14. F. Lagnel, B. Poumellec, J.P. Thomas, A. Ziani, and M. Gasgnier: Preparation of amorphous thin films of (Ti,V)O<sub>2</sub> and (Ti,Nb)O<sub>2</sub> by R.F. sputtering. *Thin Solid Films* **176**, 111 (1989).
15. M.A. Gillespie, M. van Hest, M.S. Dabney, J.D. Perkins, and D.S. Ginley: rf magnetron sputter deposition of transparent conducting Nb-doped TiO<sub>2</sub> films on SrTiO<sub>3</sub>. *J. Appl. Phys.* **101**, 033125 (2007).
16. H. Tang, K. Prasad, R. Sanjinès, P.E. Schmid, and F. Lévy: Electrical and optical properties of TiO<sub>2</sub> anatase thin films. *J. Appl. Phys.* **75**, 2042 (1994).
17. J.D. Perkins, C.W. Teplin, M. van Hest, J.L. Alleman, X. Li, M.S. Dabney, B.M. Keyes, L.M. Gedvilas, D.S. Ginley, Y. Lin, and Y. Lu: Optical analysis of thin film combinatorial libraries. *Appl. Surf. Sci.* **223**, 124 (2004).
18. K. Okada, N. Yamamoto, Y. Kameshima, A. Yasumori, and K.J.D. MacKenzie: Effect of silica additive on the anatase-to-rutile phase transition. *J. Am. Ceram. Soc.* **84**, 1591 (2001).
19. R.D. Shannon and J.A. Pask: Kinetics of anatase-rutile transformation. *J. Am. Ceram. Soc.* **48**, 391 (1965).
20. H. Tang, R. Prasad, R. Sanjinès, and F. Lévy: TiO<sub>2</sub> anatase thin films as gas sensors. *Sens. Actuators, B: Chem.* **26–27**, 71 (1995).
21. D. Wicaksana, A. Kobayashi, and A. Kinbara: Process effects on structural properties of TiO<sub>2</sub> thin films by reactive sputtering. *J. Vac. Sci. Technol., A* **10**, 1479 (1992).
22. J.-Y. Tewg, Y. Kuo, and J. Lu: Suppression of crystallization of tantalum oxide thin film by doping with zirconium. *Electrochem. Solid-State Lett.* **8**, G27 (2005).
23. H. Hosono, N. Kikuchi, N. Ueda, and H. Kawazoe: Working hypothesis to explore novel wide band gap electrically conducting amorphous oxides and examples. *J. Non-Cryst. Solids* **200**, 165 (1996).